Available online at www.sciencedirect.com
ScienceDirect
Journal of the European Ceramic Society 29 (2009) 1529–1534
www.elsevier.com/locate/jeurceramsoc

Characterization of porous silicon nitride ceramics by pressureless sintering using fly ash cenosphere as a pore-forming agent

Yingfeng Shao, Dechang Jia *, Boyang Liu

Institute for Advanced Ceramics, Harbin Institute of Technology, Harbin 150001, China

Received 17 June 2008; received in revised form 7 September 2008; accepted 13 September 2008
Available online 28 October 2008

Abstract

A new method for fabricating porous silicon nitride ceramics has been developed by using fly ash cenosphere (FAC) with mean diameter of 87 μm as a pore-forming agent. Sintering was carried out at 1780 °C for 2 h under a nitrogen atmosphere. FAC can also act as a sintering aid besides a pore-forming agent. X-ray diffraction (XRD) and transmission electron microscopy (TEM) studies showed that $YSiO_2N$ forms instead of $Y_2Si_3O_3N_4$ when FAC is incorporated. Microstructural analysis revealed that large spherical cavities are scattered in a relative dense matrix. Porous Si_3N_4 ceramics with density of 2.17–2.30 g/cm^3, Young's modulus of 141–150 GPa and strength of 180–320 MPa were obtained by changing the FAC content.

Keywords: Sintering; Porosity; Mechanical properties; Si_3N_4

1. Introduction

Silicon nitride has been widely used to fabricate cutting tools and high-temperature structural applications due to its excellent mechanical, physical and chemical properties.[1,2] Porous Si_3N_4 ceramics with a tailored microstructure are promising high-performance materials because of such unique properties as light weight, good strain tolerance, damage tolerance and thermal shock resistance.[3–5] Traditionally, porous Si_3N_4 ceramics have been used as hot gas filters, high-temperature separation membranes, and catalyst supports. Recently porous Si_3N_4 ceramic is also attractive in electromagnetic wave penetrating materials, as a strategy to reduce dielectric constant and loss.[6]

Nowadays, various processing techniques have been developed to prepare porous Si_3N_4 ceramics. The most straightforward process is reaction sintering.[7] However, the mechanical properties of ceramics sometimes cannot meet the high reliability and performance specifications required for advanced engineering applications due to high porosity. Another method to adjust the porosity is partially sintering which results in a relatively low porosity (<60 vol.%).[8] Porous Si_3N_4 ceramics can also be prepared by organic pore-forming agent method.[9] But a heat treatment is required to remove the agents, which is generally difficult to completely eliminate the impurity of residual carbon for large bulk ceramics. Consequently, each process results in unique microstructures and properties with various amounts of porosities. For the demand of particular properties of ceramics, it is crucial to control the porosity, pore morphology and size distribution.

In the present study, porous Si_3N_4 ceramics were fabricated using fly ash cenosphere (FAC) as a pore-forming agent. During sintering, FAC was melted and take an effect as a sintering aid. So finally it vanished away and pores with the same sizes of FAC retained in the matrix. In this way, pore size can be controlled by adding different size grades of FAC. And we investigated the microstructures and mechanical properties of the ceramics as a function of volume fraction of FAC.

2. Experimental procedure

2.1. Materials processing

FAC with a mean diameter of 87 μm (Yaodian fly ash Co., Pingdingshan, China), which is aluminosilicate-based hollow

* Corresponding author. Tel.: +86 451 86414291; fax: +86 451 86414291.
E-mail address: dcjia@hit.edu.cn (D. Jia).

0955-2219/$ – see front matter © 2008 Elsevier Ltd. All rights reserved.
doi:10.1016/j.jeurceramsoc.2008.09.012

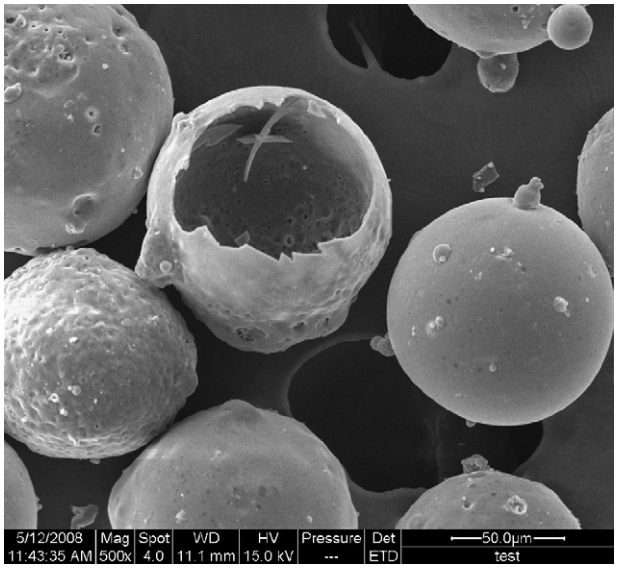

Fig. 1. SEM image of the as-received FAC indicating circular morphology and typical size.

ceramic particle, mainly composed of $Al_6Si_2O_{13}$, SiO_2 and glass phase, as shown in Fig. 1 and Table 1. The true particle density is around 600 kg/m^3 and diameters vary from 60 μm to 120 μm. The density of the ceramic material forming FAC is around 2650 kg/m^3.

The starting powder consisted of a mixture of 92 wt.% Si_3N_4 (α ratio >93%, oxygen <1.5%, particle size 0.5 μm) and 6 wt.% Y_2O_3 + 2 wt.% Al_2O_3 as sintering aids were ball-milled in ethanol for 24 h. The dry powder was sieved (90 μm) and then mixed with 5 vol.%, 10 vol.%, 20 vol.% and 30 vol.% of FAC using a mechanical stirrer for 2 h. One batch free of FAC was also prepared as a reference sample.

The mixed powder was uniaxially pressed at 20 MPa into pellets and then isostatically pressed at 150 MPa. Finally, the pellets were packed in a powder bed with a composition of Si_3N_4 + 50 vol.%BN in graphite crucibles and sintering was carried out in a gas pressure furnace at 1780 °C for 2 h under a pressure of 0.1 MPa in a nitrogen atmosphere.

2.2. Materials characterization

Bulk density was calculated from measured dimension and weight. Flexural strength was measured on a mechanical testing machine (Shimadzu, AG-Is50) using bar samples

Table 1
Typical chemical composition of FAC in weight percent.

Chemical composition of the FAC	Weight percent (%)
SiO_2	62.2
Al_2O_3	29.7
Fe_2O_3	3.5
TiO_2	1.2
CaO	0.9
K_2O	1.7
Balance	0.8

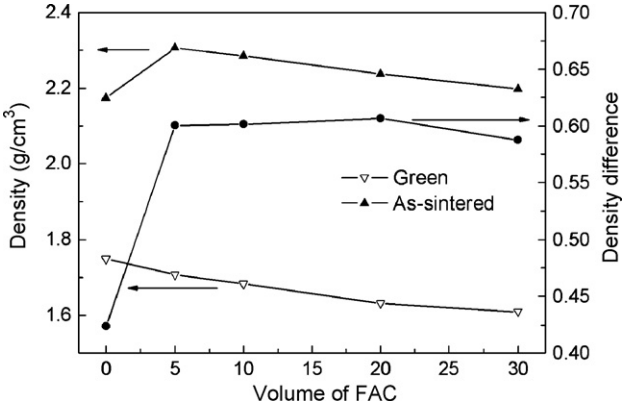

Fig. 2. Variations in the density before and after sintering versus FAC content.

36 mm × 4 mm × 3 mm on a three-point bending fixture with a span length of 30 mm and a cross-head speed of 0.5 mm/min. Young's modulus was determined from the stress–strain curves obtained from load versus deflection plot. Crystalline phases were identified by X-ray diffractometry (XRD, Rigaku, RINT-2000), using Cu Kα radiation at 40 kV and 30 mA. The microstructure was characterized by scanning electron microscopy (SEM, FEI, Quanta-200) and transmission electron microscopy (TEM, Philips, CM-12), operated at 120 kV. Pore size distributions of as-sintered ceramic samples were determined by a mercury porosimetry (Model Autopore IV 9500, Micromeritics, Norcross, GA, USA) and quantitative image analysis of cross-section SEM micrographs.

3. Results and discussion

3.1. Density

Variations in density of green and sintered bodies with different content of FAC are shown in Fig. 2. The density of green bodies decrease with increase of FAC content, and the density of all samples sintered are ranging from 2.17 g/cm^3 to 2.30 g/cm^3. Clearly, density difference between the green and sintered bodies sharply increase at early stage with FAC content,

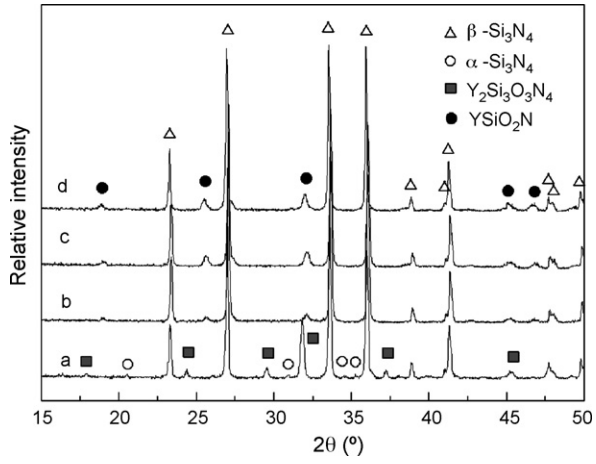

Fig. 3. XRD patterns of porous Si_3N_4 ceramics sintered at 1780 °C with different volume of FAC: (a) 0 vol.%, (b) 5 vol.%, (c) 10 vol.%, and (d) 30 vol.%.

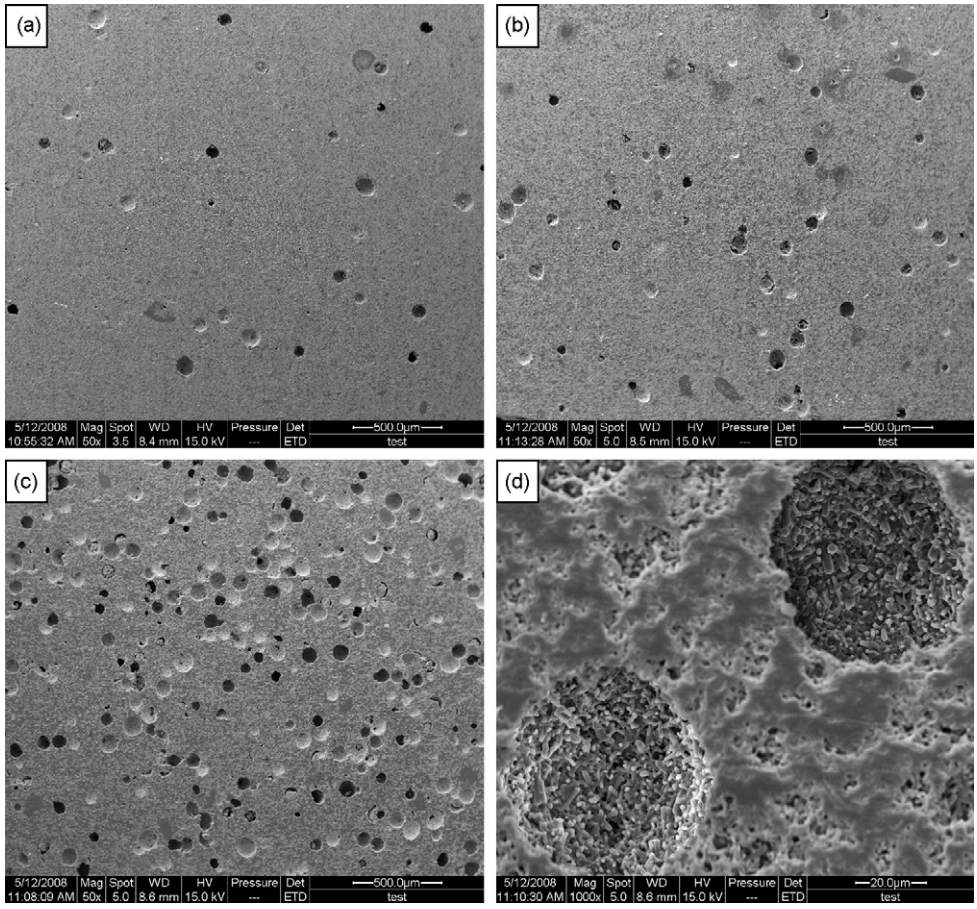

Fig. 4. SEM cross-section micrographs of porous Si_3N_4 ceramics with (a) 5 vol.% FAC; (b) 10 vol.% FAC; (c) 30 vol.% FAC; (d) small pores in matrix and spherical cavities at high magnification.

as stated above, main chemical compositions of FAC are SiO_2 and Al_2O_3 which could serve as sintering aids and promote densification. On the other hand, increasing the FAC content to 30 vol.% lead to a slight decrease in density difference. It can be attributed to the hollow structure of the FAC, the more content of it added, the more spherical-shaped pores inherited from FAC were introduced, which inhibited densification of the samples. Thus, density difference increase with the volume of FAC, and had a maximum value of 0.61 g/cm^3 with 20 vol.% FAC.

3.2. Phase composition and microstructure

The XRD patterns the porous Si_3N_4 ceramics without and with different content of FAC sintered at 1780 °C are shown in Fig. 3. As it indicated, any starting phases of FAC are no longer observed and the main phase in all samples is β-Si_3N_4. $Y_2Si_3O_3N_4$ and α-Si_3N_4 are found in FAC-free samples. With addition of FAC, the two phases vanish and another phase, $YSiO_2N$, appears instead. It can be explained that $Y_2Si_3O_3N_4$ (Y_2O_3:Si_3N_4 = 1:1) was precipitated from the Y–Si–Al–O–N glass consisted of Si_3N_4, SiO_2, Y_2O_3 and Al_2O_3.[10] When FAC was introduced, it was melted and dissolved into Y–Si–Al–O–N liquid system at high temperature,[11] which increased the silicon and oxygen content in the liquid system. Consequently it promoted the precipitation of $YSiO_2N$ (Y_2O_3:SiO_2:Si_3N_4 = 2:1:1), which is quite similar to what was reported by Yokota et al. in Y_2O_3 doped Si_3N_4 ceramics.[12] In addition, more sintering additive liquid accelerated the phase transformation of α to β silicon nitride simultaneously,[7] as expected.

SEM micrographs of cross-sections of the porous Si_3N_4 ceramics with 5 vol.%, 10 vol.% and 30 vol.% FAC are provided in Fig. 4. As shown, large spherical cavities are scattered in a relative dense matrix with a lot of small pores. And elongated β-Si_3N_4 grains oriented randomly are shown clearly (Fig. 4(d)) in inner surface of the large spherical cavities. The number of cavities and the contacting probability between them significantly increase with increasing of FAC content. At the same time, few segments of FAC can be seen as it was melted and turned into grain boundary phases during sintering process.

Fig. 5 shows the pore size distribution of the porous Si_3N_4 ceramic measured by mercury porosimetry, and it could be seen that the pore size distribution of the sintered sample is very uniform. With the increase in FAC content, median pore diameter is concentrated at 630 nm, 530 nm, 600 nm and 800 nm, respectively, indicating the small pores inside matrix which were caused by partial sintering. According to Fig. 2 and Fig. 5, both median pore diameter and density have the same trend with the increase of FAC content, suggesting a relationship between density and median pore diameter, the higher relative density, the smaller median pore diameter.

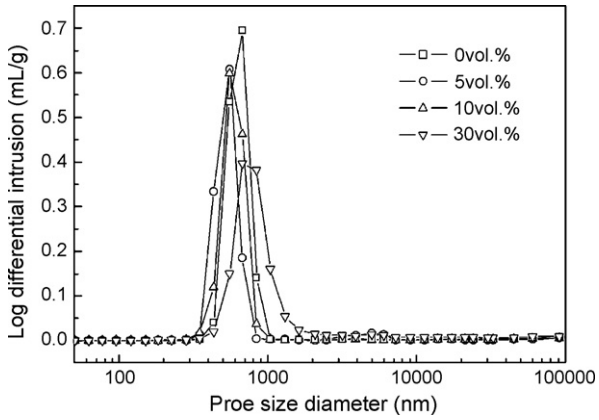

Fig. 5. Pore size distribution of porous Si_3N_4 ceramic with different volume of FAC.

Cavity size distributions obtained by using quantitative image analysis of cross-section SEM micrographs are presented in Fig. 6. The distributions of all samples sintered have no obvious difference between each other. Whereas the 30 vol.% FAC sample shows the presence of slightly bigger cavities which may be attributed to the less sintering shrinkage during densification as indicated in Fig. 3.

TEM image of 30 vol.% FAC dopped Si_3N_4 ceramic is shown in Fig. 7(a). It reveals that isolated grain boundary phases are distributed between elongated β-Si_3N_4 matrix grains, and no α-Si_3N_4 grains were observed, which is consistent with the XRD results. Additionally, $YSiO_2N$ and amorphous phase were also detected between Si_3N_4 grains in the M and N region of Fig. 7(a), respectively, as proved by the select area electron diffraction pattern (SAED) (Fig. 7(b) and (c)). Energy dispersive spectrum (EDS) analysis suggests that the amorphous phase is Y–Si–Al–O–N oxynitride glass, as shown in Fig. 7(d), which is similar to what was reported by Lee et al. in Y_2O_3 and Al_2O_3 doped Si_3N_4 ceramics.[10]

3.3. Mechanical properties

Flexural-strength and density values of the samples as functions of FAC content are shown in Fig. 8. The strength decreases with the increase of FAC content. From Fig. 8, we can see that density of the sample added 5 vol.% FAC is higher than that of the sample free from FAC, however the flexural strength is much lower, which is not consistent with the empirical relation that flexural strength increased with density. This phenomenon in the tensile and flexural strengths of brittle ceramic materials can be explained with the Griffith equation:

$$\sigma = \sqrt{\frac{ER}{\pi c}} \quad (1)$$

Tensile cracking stress (σ) is related to an effective critical crack length (c) (which may be a pore); Young's modulus (E), and fracture surface energy (R) being taken as material constants. The strength values decreased with increasing of flaw size. According to SEM micrographs of cross-sections of the porous Si_3N_4 ceramics, large spherical cavities that debase the strength are on the surface of flexural-strength samples, and it is similar to what was reported by Birchall et al. in porous cements.[13] In addition, effective critical crack length may increase with the contacting probability between cavities as FAC content increasing, furthermore, the densities are basically contributed to the strength, so flexural-strength decreased with the increase of FAC volume.

The Young's modulus and density values of the samples as functions of FAC content are shown in Fig. 9. We can see that

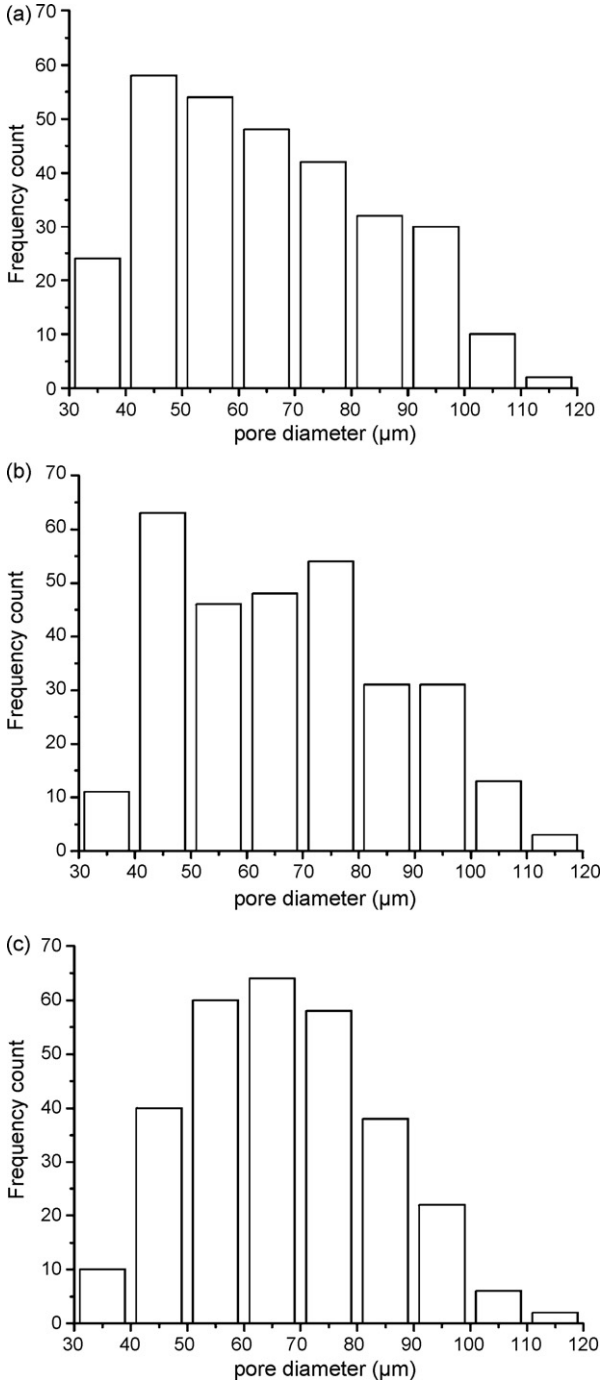

Fig. 6. Cavity size distributions obtained by using quantitative image analysis of cross-section SEM micrographs of (a) 5 vol.% FAC; (b) 10 vol.% FAC; (c) 30 vol.% FAC.

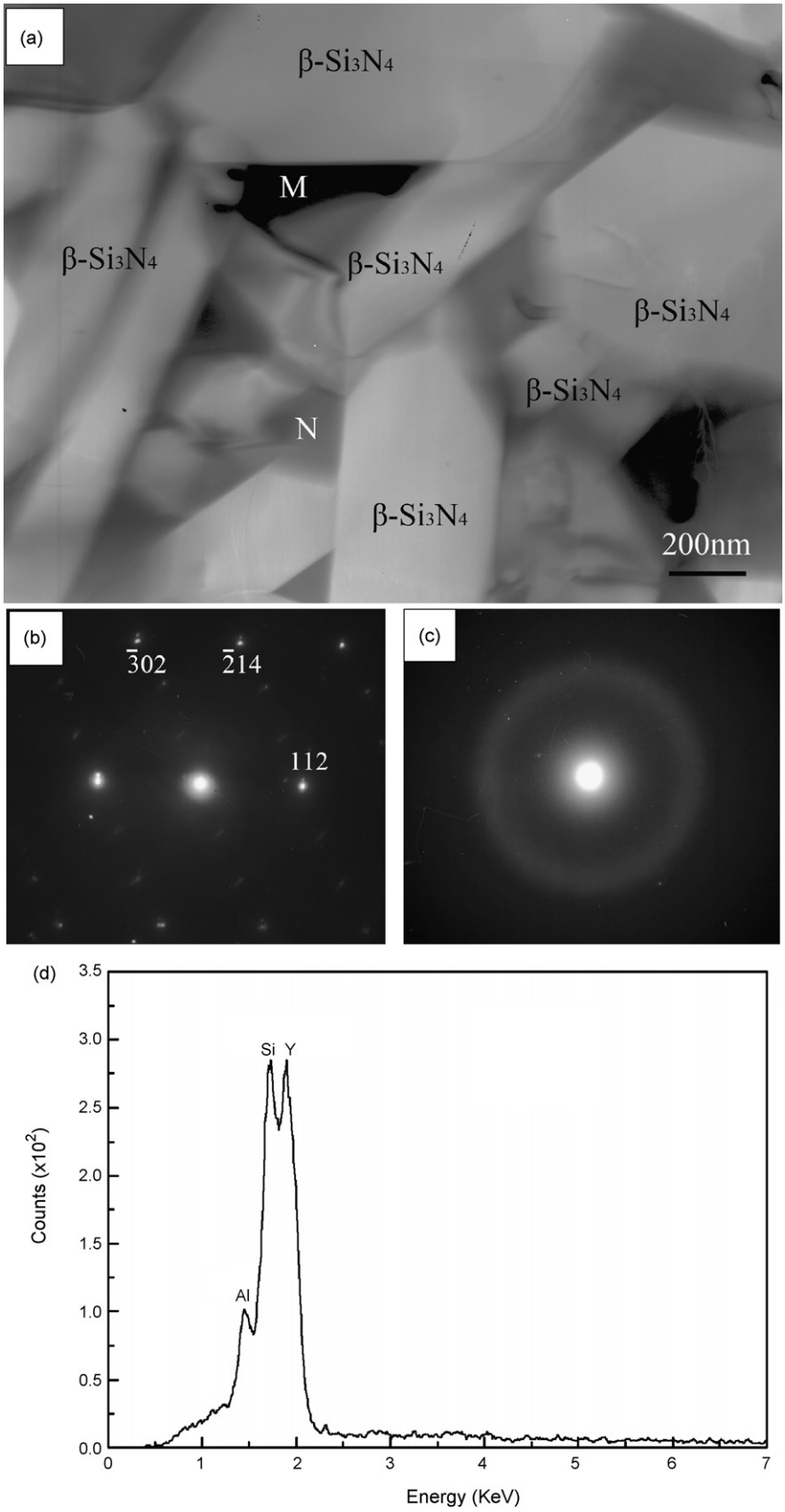

Fig. 7. (a) TEM micrograph of 30 vol.% FAC dopped Si_3N_4 ceramic, showing rod-like Si_3N_4 grains and grain boundary phase; (b) SAED of $YSiO_2N$ in M region of image (a); (c) SAED of the amorphous phase in N region of image (a); (d) EDS spectra of the amorphous phase.

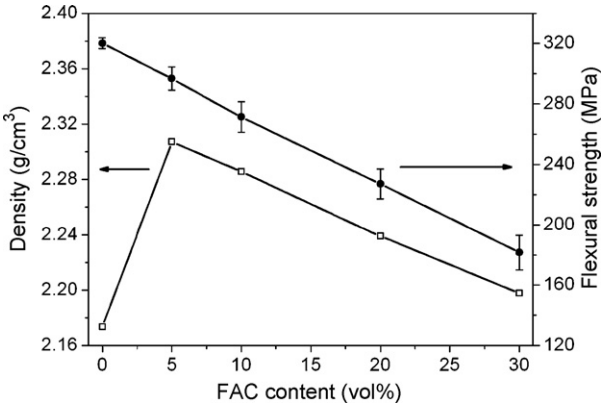

Fig. 8. Variations in flexural-strength and the density values versus FAC content.

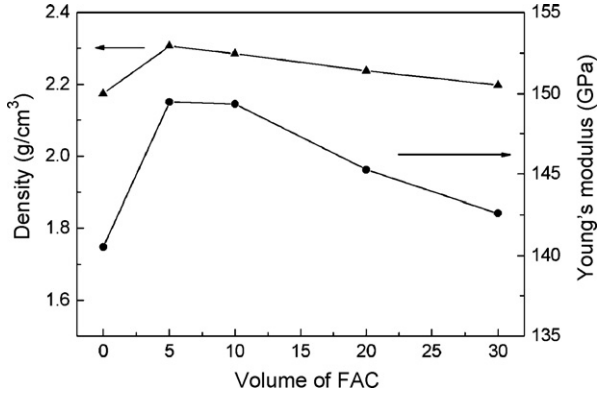

Fig. 9. Variations in Young's modulus and the density values versus FAC content.

Young's modulus values have the same trend with the density and it is consistent with numerous empirical relations which have been proposed to relate the elastic modulus to the porosity, such as simple linear relation, exponential relationship and other forms. So it is indicated that large spherical cavities on the surface of flexural-strength sample do not debase elastic modulus comparing with flexural-strength.

4. Conclusions

Porous Si_3N_4 ceramic has been fabricated at 1780 °C using fly ash cenosphere (FAC) as the pore-forming agent and FAC also acted as a sintering aid to promote the densification of the Si_3N_4 ceramic. Microstructural analysis revealed that large spherical cavities are scattered in a relative dense matrix with a lot of small pores. X-ray diffraction and transmission electron microscopy studies showed that $YSiO_2N$ appears instead of $Y_2Si_3O_3N_4$ when FAC was incorporated. The large spherical cavities on flexural-strength sample surface that debased the strength, notwithstanding the density of the FAC added sample was higher than FAC-free sample.

Acknowledgements

This work was supported by the National Natural Science Foundation of China (NSFC, Grant No. 90505011), Program of Excellent Team in Harbin Institute of Technology and the Science Fund for Distinguished Young Scholars of Heilongjiang province.

References

1. Jack, K. H., Review sialons and related nitrogen ceramics. *J. Mater. Sci.*, 1976, **11**, 1135–1158.
2. Riley, F. L., Silicon nitride and related materials. *J. Am. Ceram. Soc.*, 2000, **83**, 245–265.
3. Inagaki, Y., Ohji, T., Kanzaki, S. and Shigegaki, Y., Fracture energy of an aligned porous silicon nitride. *J. Am. Ceram. Soc.*, 2000, **83**, 1807–1809.
4. Shigegaki, Y., Brito, M. E., Hirao, K., Toriyama, M. and Kanzaki, S., Strain tolerant porous silicon nitride. *J. Am. Ceram. Soc.*, 1997, **80**, 495–498.
5. Kawai, C. and Yamakawa, A., Effect of porosity and microstructure on the strength of Si_3N_4: designed microstructure for high strength, high thermal shock resistance, and facile machining. *J. Am. Ceram. Soc.*, 1997, **80**, 2705–2708.
6. Li, J. Q., Luo, F. D., Zhu, M. and Zhou, W. C., Preparation and dielectric properties of porous silicon nitride ceramics. *Trans. Nonferrous Met. Soc. China*, 2006, **16**, 487–489.
7. Chen, D. Y., Zhang, B. L., Zhuang, H. R. and Li, W. L., Combustion synthesis of network silicon nitride porous ceramics. *Ceram. Int.*, 2003, **29**, 363–364.
8. Yang, J. F., Deng, Z. Y. and Ohji, T., Fabrication and characterisation of porous silicon nitride ceramics using Yb_2O_3 as sintering additive. *J. Eur. Ceram. Soc.*, 2003, **23**, 371–378.
9. Diaz, A. and Hampshire, S., Characterisation of porous silicon nitride materials produced with starch. *J. Eur. Ceram. Soc.*, 2004, **24**, 413–419.
10. Lee, J. S., Mun, J. H., Han, B. D., Kim, H. D., Skin, B. C. and Kim, S., Effect of raw-Si particle size on the properties of sintered reaction-bonded silicon nitride. *Ceram. Int.*, 2004, **30**, 965–976.
11. Ozcivici, E. and Singh, R. P., Fabrication and characterization of ceramic foams based on silicon carbide matrix and hollow alumino-silicate Spheres. *J. Am. Ceram. Soc.*, 2005, **88**, 3338–3345.
12. Yokota, H. and Ibukiyama, M., Effect of lattice impurities on the thermal conductivity of beta-Si_3N_4. *J. Eur. Ceram. Soc.*, 2003, **23**, 55–60.
13. Birchall, J. D., Howard, A. J. and Kendall, K., Flexural strength and porosity of cements. *Nature*, 1981, **289**, 388–390.